TOWARDS A NEW DIAGNOSIS AID OF CARDIOVASCULAR DISEASES USING 2D-MULTIMODAL DATA REGISTRATION AND 3D-DATA SUPERIMPOSITION

G.Valet[1,2], S. Sanchez[1], J.M. Lopez-Hernandez[1], Ch. Daul[1], D. Wolf [1] and G. Karcher [3]

[1] Centre de Recherche en Automatique de Nancy (CRAN, CNRS UMR 7039)
2 avenue de la Forêt de Haye, 54516 Vandœuvre-Lès-Nancy, France
[2] Segami, 22 rue Sibelle, Paris, France
[3] Laboratoire d'Insuffisance Cardiaque: Mécanimes Physiopathlogiques et Thérapeutiques EA 2403, CHU de Nancy, 54511 Vandœuvre-Lès-Nancy, France.

ABSTRACT

This contribution deals with the diagnostic aid for cardiovascular diseases using a simultaneous exploitation of nuclear medicine imaging and X-ray cine angiography. The aim of this work is to build both a 2D and a 3D-representation of the superimposition of the coronary tree (stemmed from X-ray angiography) with the myocardial perfusion data (obtained with single-photon emission computed tomography). These new images lead to a better understanding of the relationship between arterial stenosis and consequences on myocardium perfusion. The 2D-registration of the two modalities is first presented. The 3D-reconstruction of vessels using multiple angiographic viewpoints is then developed. Tests performed on a phantom showed that the mean distance between the back projections of 3D-reconstructed artery points into the coronarographies and the corresponding initial 2D-points used by the 3D-reconstruction equals 6 mm. Similar results were obtained for five patients.

1. INTRODUCTION

The diagnosis of heart diseases is notably based on the analysis of myocardium perfusion and ischemia observed on tomoscintigraphic images obtained from single photon emission computed tomography (SPECT). These data give 3D-informations about myocardial perfusion with a voxel resolution of 5 mm by 5 mm by 5 mm. The 2D and 3D-fusion of coronarographic data (providing images of the artery tree) with SPECT-data facilitates the diagnosis of heart diseases. In 2D, two mirror views of the same coronarography coloured with the perfusion data of two opposite heart sides are determined. This 2D-representation allows the cardiologist to focus on regions of interest without disturbing the expert's coronarography lecture. However, the link between arterial stenosis and insufficient blood supply can not be explicitly established in 2D. To obtain this link a complementary 3D-representation is realized. The latter representation visualizes the schematically reconstructed artery tree set onto the 3D-perfusion volume. This 3D-synthetic image permits to localize the stenosis marked by a specialist in the 2D-images with regards to perfusion defaults. Both 2D and 3D-data superimposition methods are based on the 2D-registration of the data of the two modalities. This registration algorithm and the principle of the 3D-reconstruction of the schematic artery tree are presented in the next section.

The work described in this paper was partially sponsored by SegamiCorporation[2] and the ANVAR organization.

2. METHODOLOGY

Knowing the angle of view of the coronarographies it is possible to project the SPECT-data into planes parallel to those of the X-ray angiographies. A registration algorithm is used to find the parameters of the rigid transformation T permitting the superimposition of the projected SPECT-data onto the coronarographies using T^{-1} . The myocardium edges are the homologous structures on which the registration algorithm is based. Particular points (e.g. artery segments beginnings, ends or bifurcations) are marked on the X-ray images. The transformation T is used to compute the positions of the previous points in the planes of the projected SPECT data. An orthogonal projection model is then employed to reconstruct the homologous points onto the 3D-perfusion data. The principle of the algorithm is sketched in Fig. 2 and summarized in this section.

2.1. Myocardium segmentation

The edges of the SPECT-modality are well defined and can simply be segmented using a classical edge detector and a global threshold method. The edges of the X-ray images are, on the other hand, poorly contrasted and affected by strong noise. These images are first treated with the edge detector of Deriche [1]. Edge parts are then selected according to criteria like length, curvature and mean grey-level value of the edge parts. These selected contours are used to compute a distance map [2], each value of this image giving the shortest distance of the corresponding image point to the closest edge part. The distance map acts as an external

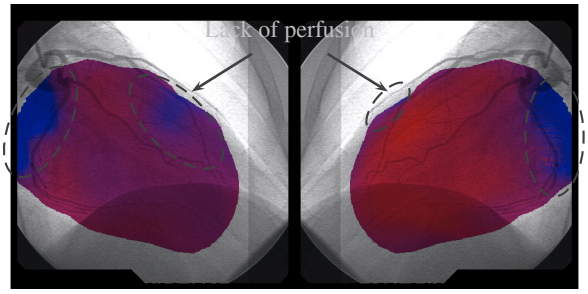

Fig. 1: **Patient 4 : Right Anterior Oblique (RAO) projection of 30°. Mirror coronarographic views with the associated myocardial perfusion data from tomoscintigraphy. In the SPECT-data, the lack of perfusion appears in blue whereas a normal perfusion is visualized in red.**

energy attracting a contour (snake [3]). The initialization of the latter is either manual or based on the myocardium contour of the SPECT-modality. An internal energy (based on *a priori* knowledges like myocardium contour shape and size) controls the snake displacement. This algorithm led to a robust edge segmentation method.

2.2. Data registration

The segmented edge of the SPECT-modality is used to compute a distance map which represents the model data in the proposed registration scheme. A rigid transformation is applied to the contours of the angiographic X-ray modality. The similarity measure S, representing the degree of superimposition of the contours of the two modalities, is given by the arithmetic mean value of the distance map pixels values superimposed with the angiographic contour. By minimizing S with a simplex algorithm, it is possible to find the transformation T superimposing the two contours. The transformation T^{-1} is then used to determine the 2D-data fusion representation (see Fig. 1). The segmentation and registration algorithms are detailed in [4] and [5].

2.3. Schematic reconstruction of the artery tree

As sketched in step 1 of Fig. 2, the SPECT-data are projected in planes which are parallel to the image planes of the available coronarographies. The mathematical link between the coordinate systems $(O_t^i, \overrightarrow{x}_t^i, \overrightarrow{y}_t^i)$ of the SPECT-planes –corresponding to the angles of view i– and a 3D-patient coordinate system $(O_p, \overrightarrow{x}_p, \overrightarrow{y}_p, \overrightarrow{z}_p)$ in which the 3D-SPECT data are given, is exactly known. Points describing the artery tree (beginning, end and bifurcations of artery segments) and particular point (e.g. stenosis) are then marked on the coronarographies (step 3). The corresponding positions are known in the coronarography coordinate systems $(O_c^i, \overrightarrow{x}_c^i, \overrightarrow{y}_c^i)$. The transformation T, obtained with the segmentation (step 2) and the registration (step 4) permits to determine the positions of the marked points in the SPECT-plane coordinate systems (step 5). The coordinates of the homologous points are then computed in $(O_p, \overrightarrow{x}_p, \overrightarrow{y}_p, \overrightarrow{z}_p)$ (step 6) and reconstructed in 3D (step 7). The correspondence between homologous points is established by a

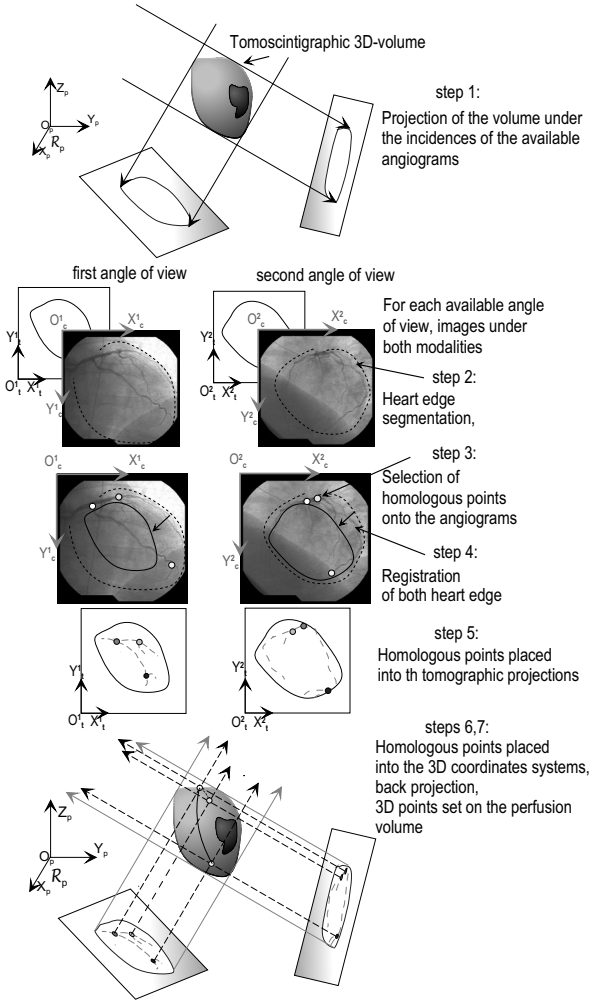

Fig. 2: **3D-data superimposition (illustration with only two angles of view). The dotted lines in the coronarographies (step 2) represent the segmented myocardium edges. The continuous lines of step 4 correspond to the myocardium edges of the SPECT-planes projected directly into the coronaropraphies. The contour points of the doted and continuous lines are registered for finding the transformation T.**

specialist during the point marking on the coronarographies thanks to a friendly user interface.

An artery tree is built by projecting back (doted lines of step 7 of Fig. 2) the homologous points of step 6 and by computing the intersection points of the corresponding 3D-lines. Criteria like accuracy, simplicity (the habits of the manipulators should not be changed) and portability (the method might be free from any specific geometry of the acquisition system) were fixed for the development of the reconstruction algorithm. The real projection model of a coronarograph is conical since the X-ray source is quasi punctual. This projective model requires a precise knowledge of the sensor geometry (the latter changes from one coronarograph to another and for each viewpoint) and is hence system dependent. Moreover, for many coronarographs the exact geometry is unknown (a calibration step, needed for each sensor position and delivering the geometrical param-

eters of the acquisition system, should be avoided). For all these reasons an orthogonal model was chosen. This model represents an accurate approximation of a projective model since the heart is close to the image plane and about one meter away from the X-ray source. As demonstrated in the result section, inaccurate projective parameters (mean distances between X-ray source positions, estimated patient's heart positions and image planes were computed for several table positions and used in the projective model) lead to less accurate reconstructions than with an orthogonal projection model. The selected artery points are 3D-reconstructed by determining in $(O_p, \overrightarrow{x}_p, \overrightarrow{y}_p, \overrightarrow{z}_p)$ the intersections of the SPECT-plane orthogonal lines passing through the marked points placed in $(O_t^i, \overrightarrow{x}_t^i, \overrightarrow{y}_t^i)$. Due to the patient heart movement, the difference of myocardium edge localization in the two modalities (true edge in end of diastole in the X-ray images and mean outline in tomography, see Fig. 4), the registration inaccuracy and the imprecision of artery point marking the 3D-lines of the different viewpoints do not intersect exactly. The intersection point of N 3D-lines is computed thanks a least mean square resolution of an over-determined system. The best point with respect to the criterion of least squares is taken as intersection point of the N lines. In fact, due to the reasons mentioned previously, the reconstructed 3D-points do not lie exactly on the surface of the 3D-perfusion data. To overcome this problem, the reconstructed points are projected onto the nearest point of the 3D-perfusion volume. The mean distance between the latter and the 3D-points is about 3 mm.

3. EXPERIMENT AND RESULTS

To evaluate the accuracy of the 3D-reconstruction and of the setting of the schematic tree onto the perfusion volume, the 3D-points are projected again into the coronarographies. The distances between the projected points and the original ones selected by the specialist are then computed. This protocol was performed with the phantom shown in Fig. 3, the corresponding results being given in Table 1.

Fig. 3: **Heart phantom. It is a structure made of PMMA (Poly Methyl MethAcrylate) which approximates the shape of a heart thanks to a cylinder having a half-sphere put on it. Such two cylinders form a double hull in which a radioactive tracer can be introduced for simulating the examination of tomoscintigraphy. A metallic tree, opaque to X-rays, is set onto the surface of the external cylinder and of the half-sphere to obtain the examination of coronarography.**

3D-reconstruction model	Mean error in pixels (in mm)
Orthogonal modelling and exact geometric heart edge	6.16 (2.46)
Orthogonal modelling and mean heart edge	10.02 (4)
Conical modelling and exact geometric heart edge	7.08 (2.8)
Conical modelling and mean heart edge	11.28 (4.5)

Table 1: **Reconstruction results for 17 angiographic angle of views acquired for the phantom of Fig. 3. Four 3D-reconstruction models were obtained by combining either a conical or orthogonal projection and by using either the exact geometric heart edge or a mean edge from the Mirage software (standard software used by clinicians and delivering 3D-perfusion data).**

The software (Mirage), used by the clinicians, delivers data corresponding in fact to a 3D-mean contour of the cardiac muscle (heart wall of Fig. 4). The results of Table 1 demonstrate that exact 3D-contours of the myocardium lead to a more accurate 3D-reconstruction than the mean contour, whatever the geometrical model used for the tomograph. The latter observation can be explained by the fact that the registration is more accurate with the exact 3D-contour computed with the SPECT-data. Table 1 confirms also that the orthogonal projected model lead to better reconstruction results than a projective model with approximately known parameters.

Three parameters influence strongly the 3D- reconstruction accuracy, namely the zoom factor during the coronarographic acquisition, the number of viewpoints used for the reconstruction and the distribution of the angles of view (rather close angles of view, well distributed orthogonal viewpoints or a mix of close and well distributed viewpoints). Fig. 5 summarizes the results obtained by giving different values to the three latter parameters. The zoom factor of the data set "data 1" is smaller than the one of data set "data 2". One can observe in Fig. 5 that for a large zoom factor or/and for well distributed viewpoints, the reconstruction accuracy is best and is independent from the number of viewpoints. For a lower zoom factor and for redundant or close angles

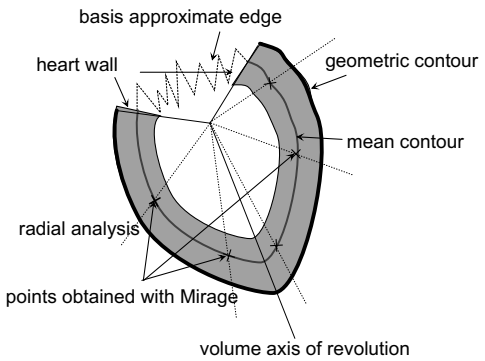

Fig. 4: **Difference between an exact myocardium contour and the mean heart contour given by Mirage software.**

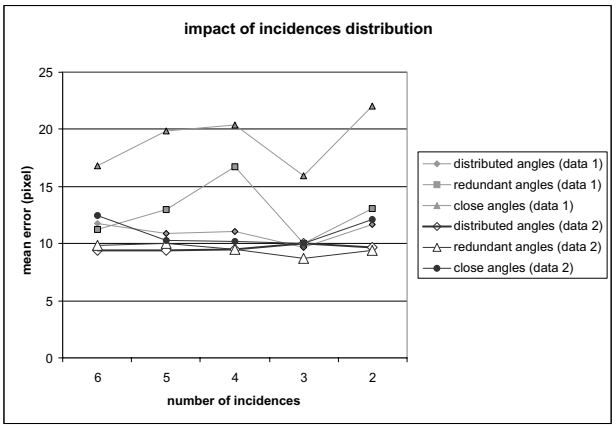

Fig. 5: **Impact of number and distribution of available angles. "Redundant" describes a distribution with both close and well distributed angles. This situation is the most common one in real cases.**

the accuracy of the proposed algorithm is lower and dependents on the viewpoint number. The worst error obtained with the phantom (see Fig. 5) is about twenty pixels, representing a mean distance of 5 mm between marked and back projected points.

Results obtained with data of five patients confirm those previously presented for the phantom. Data of one patient led to particularly good results (mean error of 7.7 pixels / 2 mm). For this patient, the registration delivered optimal results and only two well-dispatched viewpoints were available. For the other four patients, the results were also satisfying since the mean distance between marked and back projected points was about 30 pixels (6 mm).

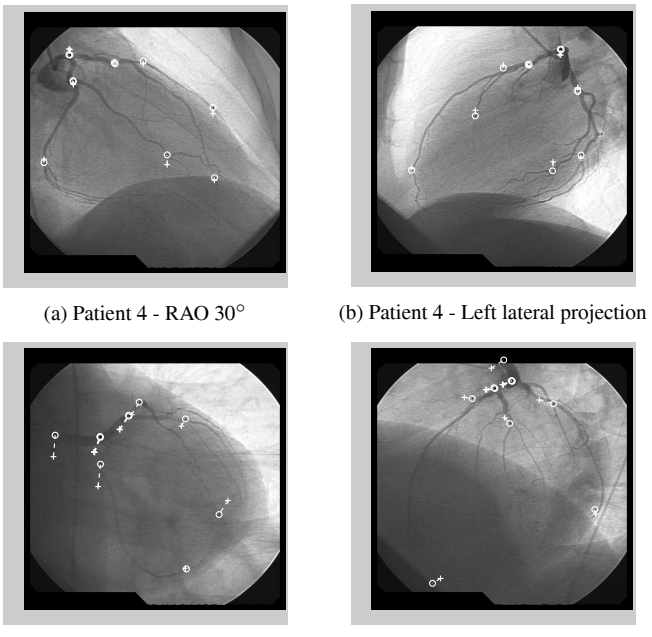

(a) Patient 4 - RAO 30°

(b) Patient 4 - Left lateral projection

(c) Patient 2 - RAO 0°, Caudal 30°

(d) Patient 2 - LAO 60°, cranial 20°

Fig. 6: **Error evaluation of the reconstruction method for two patients. Initial homologous marked points are visualized by circles and the reconstructed and back projected points are represented by crosses.**

Fig. 7: **3D-representation for patient 4. This representation can rotate and can hence be seen under any viewpoint.**

One can notice here that the voxel size of the SPECT-data is 5 mm by 5 mm by 5 mm whereas the pixels of the coronarographies are 0.5 mm squares. With these resolutions, the results obtained for the patients with the proposed algorithm are judged acceptable by the clinicians. Moreover, knowing that the heart is in movement during data acquisition, that for normal pathological cases the perfusion volume is lacunary, *etc.* the algorithm seems to be robust and accurate enough.

The 2D-mirror representation, the superimposition of the schematic 3D-artery tree onto the SPECT-data and the reconstruction error measures are respectively given in Fig.1, Fig. 6 (a),(b) and Fig. 7 for the patient with the best results (patient 4). The reconstruction error is also given in Fig. 6 (c),(d) for one of the four other patients (patient 2, most representative case).

4. CONCLUSION

The method of reconstruction presents the advantage of using standard examinations without important changes in the clinical procedures and without any specific strong constraints (only the heart centering in the coronarography examination is needed).

The 3D-model enables the clinician to see clearly the link between a given artery segment and the associated perfusion data. The mean error of 3D-reconstructed points projected again in 2D- coronarography images is about 6 mm.

The 3D-model and 2D-superimposition are completely realistic and represents a useful solution for the diagnosis of cardiovascular diseases.

5. REFERENCES

[1] R. Deriche, "Using canny's criteria to derive a recursively implemented optimal edge detector," *International Journal of Computer Vision*, vol. 1, no. 2, pp. 167–187, May 1987.

[2] G. Borgefors, "Distance transformations in digital images," *Computer Vision, Graphics, and Image Processing*, vol. 34, pp. 344–371, 1986.

[3] M. Kass, A. Witkin, and D. Terzopoulos, "Snakes: active contour models," *International Journal of Computer Vision*, vol. 1, no. 4, pp. 321–331, 1988.

[4] S. Sanchez, G. Valet, Ch. Daul, D. Wolf, and G. Karcher, "Registration of cardiac tomoscintigraphy data and coronarography data," in *Proc. of the 2nd European Medical and Biological Engineering Conference EMBEC'02*, Vienna, Austria, December 2002, vol. 3, pp. 946–947.

[5] S. Sanchez, G. Valet, J.M. Lopez-Hernandez, D. Wolf, Ch. Daul, and G. Karcher, "2D and 3D-superimposition of cardiac SPECT and coronarography data," in *Proc. of 25th Annual International Conference of the IEEE Engineering in Medicine and Biology Society*, Cancun, Mexico, September 2003, pp. 607–610.